Ferromagnetic hcp Fe in Fe/Re(001) multilayers

F. Perjeru, M. M. Schwickert, Tao Lin, A. Anderson, and G. R. Harp
Department of Physics and Astronomy, Ohio University, Athens, Ohio 45701
(Received 29 April 1999)

Until now, the hexagonal closed-packed (hcp) phase for bulk Fe, Fe multilayers, or Fe alloys has always been associated with a paramagnetic state. We show evidence that hcp Fe can support a ferromagnetic moment in Fe/Re multilayers. The structure and magnetic properties of Fe/Re multilayers are studied using x-ray diffraction, energy dispersive x-ray analysis, magneto-optical Kerr-effect magnetometry, and x-ray magnetic circular dichroism. The Fe layer thickness t_{Fe} is maintained constant at 8 Å , while $0 \leqslant t_{Re} \leqslant 35$ Å . For $t_{Re} < 8$ Å the multilayer has a body centered tetragonal (bct) structure with a perpendicular interplanar spacing that increases with increasing Re thickness. Beyond the $t_{Re} \approx 9$ Å the structure transforms to hcp. Fe has a quite stable magnetic moment for all t_{Re}, before and beyond the structural phase transition.

I. INTRODUCTION

Among the transition metal ferromagnetic elements (Fe, Co, Ni), Fe is unusual in that it has the highest moment of the three and in that it is a weak magnet (majority *d* band is not full), whereas Co and Ni are strong magnets (full majority *d* band). The former property makes Fe containing materials useful in applications requiring a high magnetization. The latter means that the Fe moment is unstable, and varies widely ($0-3\mu_B$) depending on the details of material composition and structure.

Theoretical calculations[1–3] for fcc and bcc Fe reflect this point. Calculations confirm that in bcc arrangement the ferromagnetic (FM) state has a lower energy and a larger equilibrium volume as compared with an antiferromagnetic (AFM) or nonmagnetic (NM) state.[2] However, in the fcc structure, the FM, AFM, and NM states are almost degenerate, and the transitions between these states is lattice parameter dependent. It was calculated that for small lattice parameters AFM order is preferred, while for large lattice parameters, the energetically more favorable magnetic structure is FM. Experimentally, thin films of fcc Fe stabilized through epitaxy may be FM, AFM, or NM depending on the lattice constant and electronic interactions at the substrate interface.[4,5]

Because of the close relationship between the fcc and hcp structures, one might predict a similar variance in the magnetic behavior of hcp Fe. Indeed, while calculations of hcp Fe indicate a NM ground state,[6,7] a small increase in lattice constant induces a FM state with a moment of 2.7μB.[7] However, experiments have always associated the hcp phase of Fe with a nonmagnetic state. For example, Taylor *et al.* investigated the hcp phase of Fe stabilized under high pressure.[8] Mössbauer effect results showed that Fe is in a paramagnetic phase down to liquid-helium temperatures. Other conditions yielding an hcp Fe phase use the hcp elements Ru and Re. Fe/Re alloys cannot be prepared because they are immiscible over most of the composition range. However, hcp FeRu alloys can be prepared with relatively high Fe concentration. Yet these alloys are always paramagnetic, even up to 75% Fe concentration.[9] A study of Fe/Ru(0001) multilayers[10] shows that a magnetic moment appears when the Fe layer thickness $t_{Fe} > 8$ Å . However, by this point the Fe film has already begun phase transformation back to its stable bcc structure. Another recent study[11] showed that hcp Fe stabilized in Fe/Ru (102) multilayers has no magnetic moment.

Here we present evidence that hcp Fe may posess a magnetic moment, when the hcp phase of Fe is stabilized within Fe/Re multilayers. Epitaxial Fe/Re films are deposited on MgO(001) substrates. The quality and structure of these films is determined using x-ray diffractometry (XRD). It is found that the Fe/Re multilayers have a bct (001) ordering for $0 \leqslant t_{Re} \leqslant 8$ Å , after which a structural phase transition occurs to an hcp phase.

The magnetic properties of Fe/Re multilayers are investigated using magneto-optical Kerr-effect (MOKE) magnetometry, while element specific magnetic moment measurements were performed using x-ray circular magnetic dichroism (XMCD). XMCD analysis establishes that even after the structural phase transition from bct to hcp, the magnetic moment of Fe in Fe/Re multilayers is not affected.

II. SAMPLE PREPARATION

The films used in the study were prepared by dc magnetron sputtering in 3×10^{-3} Torr, with a deposition rate of ≈ 1 Å /s. The base pressure of the ultrahigh vacuum system is $< 5 \times 10^{-10}$ Torr. The samples were deposited with uniform Fe layers and varying Re thicknesses. In order to have consistent growth conditions, thickness wedges of Re layer varying from 0–35 Å across a 2in. substrate were deposited. The structure of the sample is as follows. A 25 Å Cr(001) film was deposited onto an MgO(001) substrate at 600 °C followed by 300 Å Cr(001) at 300 °C to seed subsequent growth. This was followed by the structure: Fe 8 Å /[Re 0–35 Å /Fe 8 Å $]_{20}$/Al 20 Å .

An optimal growth temperature of 230 °C for the multilayer was determined by growth tests at various temperatures. The final Al capping layer, deposited at room temperature, is used to protect the sample against oxidation after removal from the growth chamber.

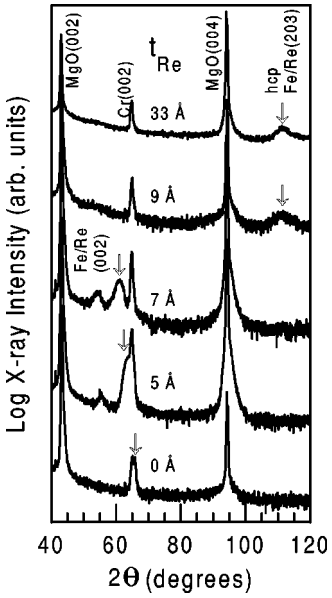

FIG. 1. Specular x-ray scans from different positions on the wedged multilayer corresponding to various t_{Re}. The largest features observed are the MgO substrate (002) and (004) peaks and the Cr buffer layer (002) peak. The primary multilayer peak (marked with an arrow) appears between 52°–68° ($t_{Re}<9$ Å) and near 112° ($t_{Re}>9$ Å). Superlattice satellites can be seen near this peak for $t_{Re}=5$–7 Å. The multilayer peak moves gradually to lower angles (larger lattice constants) with increasing t_{Re}. For $t_{Re}<9$ Å, the multilayer has a coherent bct structure. Beyond $t_{Re}=9$ Å the bct-related features disappear and are replaced with an Hcp-related feature near ≈112°.

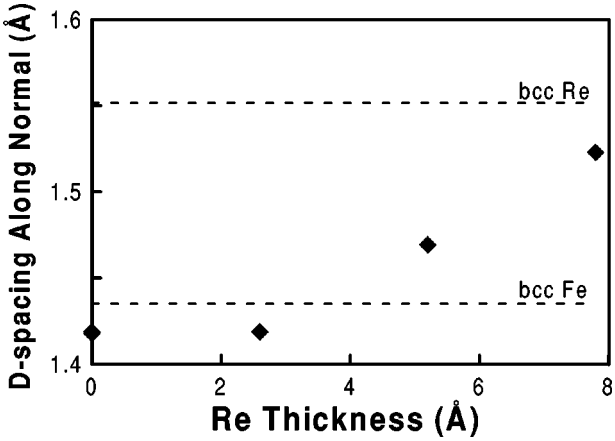

FIG. 2. Interplanar (d) spacing along the surface normal as a function of t_{Re} in the bct region. The spacing begins close to the value for Fe, and then rises monotically with increasing t_{Re}, approaching the expected value for bcc Re (if such structure existed).

III. THICKNESS CALIBRATION

The sputtering rates were calibrated by the growth of 1000 Å thick Fe and Re films, whose thickness was measured with step profilometry. Analysis of x-ray diffraction measurements (presented below) indicated bilayer repeat distances in good quantitative agreement with the nominal thicknesses of Fe and Re layers. Energy dispersive x-ray analysis in a scanning electron microscope serves as a supplemental verification of sample composition. The results agree with the expected elemental composition, namely, the chemical components found are Mg (from substrate), Cr (buffer layer), Fe, Re, and Al (capping layer). Comparing the Fe composition for different positions it was found that all samples used in this study have the same thickness of Fe within 10%. Qualitative measurements at different points on the wedge showed that the Re thickness increases linearly along the wedge, as expected.

IV. STRUCTURAL CHARACTERIZATION USING XRD

The films were characterized by high-angle x-ray diffraction (XRD). Figure 1 displays typical x-ray diffraction specular scans from different positions on the wedge. These were taken with a two-circle fixed anode diffractometer using Cu K_α radiation. The dominant features in all spectra are the MgO(002) peak near 43°, the MgO(004) peak near 94°, and the Cr(002) peak at 64.9°. The main Fe/Re multilayer features are marked by arrows in each scan. Additional superlattice satellites surrounding this feature are apparent in the $t_{Re}=5$ and 7 Å scans.

Below $t_{Re}\lesssim 8$ Å, the Fe/Re multilayers have a bct(001) crystal structure with gradually increasing lattice constant along the surface normal, as evidenced by movement of the main feature toward smaller 2θ angles. Near $t_{Re}\approx 9$ Å, the multilayer undergoes a phase transition. While the bct peak disappears, a new feature can be seen at ≈111.5° which we identify as hcp(203) (see below). Because no bcc-Fe related features are observed for $t_{Re}>9$ Å, we conclude that the Fe/Re multilayer has a locally coherent crystal structure with both Re and Fe adopting the hcp structure. This is quite similar to previous observations in hcp Fe/Ru.[11]

Using spectra such as those in Fig. 1, one can determine the average perpendicular lattice constant in the bct region of the multilayer, displayed in Fig. 2. It can be seen that for thinner Re layers the lattice structure is close to that of bcc Fe, as expected. Increasing t_{Re}, the monolayer spacing increases monotonically, up to ≈1.52 Å ($2\theta=58.58°$) for $t_{Re}=8$ Å. This is close to the lattice constant we predict for metastable bcc Re, determined by analogy between the bcc and hcp structures of Fe and Re. These results are consistent with the interpretation of a coherent bct crystalline structure in this thickness range.

Numerous off-specular radial scans and rocking curves were examined for the position on the sample corresponding to 33 Å of Re, typified in Fig. 3. These Bragg reflections correspond to no allowed Bragg reflections in either the substrate or buffer layer and are identified in the figure by indexing on an hcp lattice. From such scans, d spacings within the Fe/Re structure are identified. A summary of all the observed d spacings is found in Fig. 4 (expt.).

In order to positively identify the crystalline phase after the phase transition, the experimentally determined d spacings are compared with spacings expected for perfect unstrained bcc, fcc, and hcp ($c/a=\sqrt{8/3}$) structures. To set the lattice constant, each hypothetical structure was scaled such that its most prominent feature had a d spacing of 2.08 Å, the d spacing of the most prominent experimental feature. The d spacings within these hypothetical structures are also plotted in Fig. 4. Visual comparison shows that the hypo-

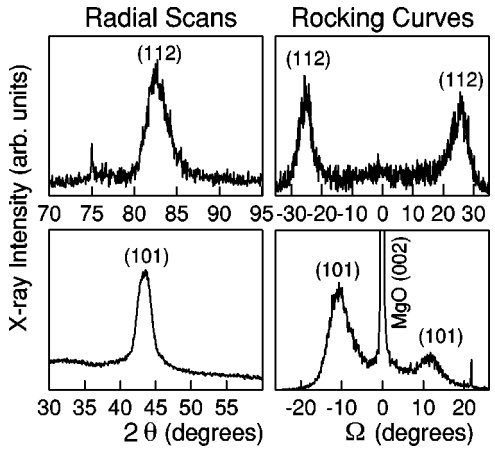

FIG. 3. Left: Radial scans from the part of the sample with $t_{Re} = 33$ Å for peaks which we index as hcp (112) and (101) (this indexing is justified in the following figure). Right: Rocking curves through the Fe/Re (112) and (101) diffraction features for the same sample. In the (101) rocking curve, the 2θ value happens to be close to the value for MgO(002), so this peak appears along the surface normal. The presence of equivalent features on either side of the surface normal indicates a multidomain structure of the film.

thetical hcp structure by far shows the best agreement with the experimental results. A least-squares fitting between the hypothetical hcp structure and our experiment yielded lattice constants of $c = 4.45$ Å and $a = 2.75$ Å. These lattice constants are slightly smaller than hcp Re ($c = 4.46$ Å and $a = 2.76$ Å), as expected.

The surface normal in the hcp region is found to be close to the [203] direction. This growth direction has a uniaxial surface symmetry, if one includes the top two layers of the

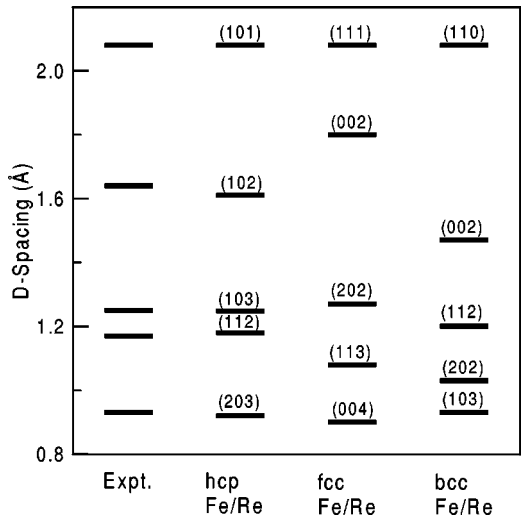

FIG. 4. From data such as those in the previous figure, a number of d spacings are determined for the $t_{Re} = 33$ sample. The experimental d-spacings are compared with predicted d spacings for hcp, fcc, and bcc lattices. The overall scaling for each structure was set by the most prominent feature at 2.08 Å. The lattice constant of each structure was adjusted so that the strongest feature within each crystal structure [hcp(101), fcc(111), bcc(110)] agreed with this value. From the good agreement between the experiment and predicted hcp values, we conclude this film has an hcp crystal structure.

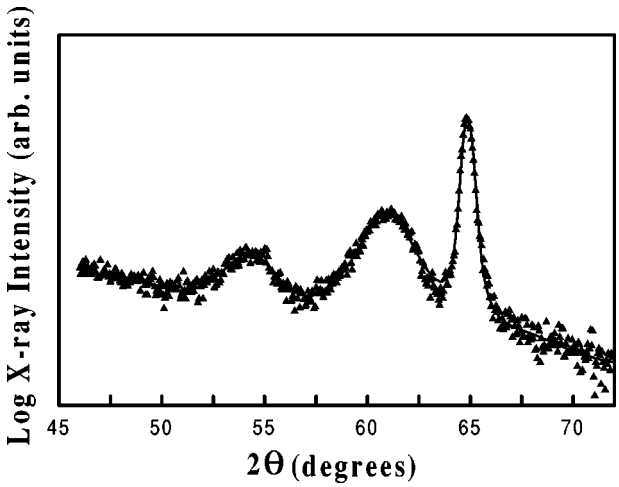

FIG. 5. X-ray fit to experimental data corresponding to a superlattice with 7 Å of Re and 8 Å of Fe. The fit is shown as the solid curve in Fig. 5.

surface. Thus, on the fourfold symmetric Cr(001) buffer layer, there are four equivalent orientations of epitaxial alignment, which leads to four domain types within the film. This multidomain structure is evidenced in the rocking curves of Fig. 3, where equivalent features are observed on either side of the surface normal (note peaks with positive ω angle often have reduced intensity due to an asymmetry in our experimental arrangement).

More specifically, the (101) rocking curve was taken in a plane aligned with the Cr(100) planes. This indicates that the hcp c-axis and the surface normal define a plane parallel to the Cr(100). The four different domains have c-axis vectors whose projections into the sample plane are aligned with the Cr(100), Cr(010), Cr($\bar{1}$00), and Cr(0$\bar{1}$0) planes. Radial scans that were taken with x-ray scattering vector not parallel to Cr(100) planes did not show Fe/Re(101) features, which demonstrates that there is an epitaxial relationship between the Fe/Re and Cr buffer layers. Similar statements are true for other Bragg reflections from the hcp structure.

Note that the expected positions of the c axis related $(00X)$ features are such that they could not be probed within the mechanical limitations of our x-ray diffractometer. Consistent with this, we saw no evidence for features related to $(00X)$ peaks in any of our scans. For this reason, the hypothetical $(00X)$ peak positions are not displayed in Fig. 4. The same statements could be made about the hcp$(X00)$ reflections.

Finally, to estimate the degree of interdiffusion between the Fe and Re we pursued calculational fitting of the specular x-ray diffraction. An example of this is shown in Fig. 5. The best fit to experimental data corresponding to a superlatice with 7 Å of Re and 8 Å of Fe with an interdiffused interface model, is shown as the solid curve in Fig. 5. The x-ray fit indicates interdiffusion in the present superlattice of ≈ 1 ML at the interfaces. This would be expected from the binary alloy phase diagram of Fe and Re. Due to the immiscibility of Fe and Re up to 75% Fe, there is also little intermixing at the interfaces in the present multilayers.

V. MOKE MEASUREMENTS

Bulk magnetic properties were characterized by magneto-optic Kerr effect. MOKE data showed easy-axis loops in the

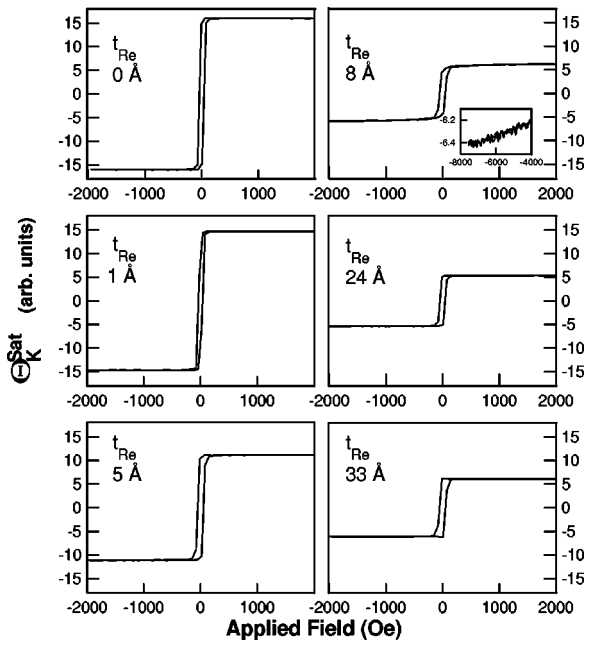

FIG. 6. Longitudinal magneto-optic Kerr effect loops taken along the easy axis of the Fe/Re wedge at different positions corresponding to different t_{Re}. Inset: The $t_{\mathrm{Re}}=8$ Å sample has a small component of material with a high saturation field, associated with disorder in the phase transition region.

bct region of these multilayers parallel to the bcc Fe[100] direction. Representative hysteresis loops are displayed in Fig. 6. It can be seen that the sample is fully saturated in relatively low applied magnetic fields except near $t_{\mathrm{Re}}=9$ Å where the film undergoes a phase transition. An inset in the $t=8$ Å graph displays the high field behavior of this loop. To bring out this point, Fig. 7(upper) displays $H_{95\%}$, the applied field required to bring the sample to 95% of saturation, plotted as a function of t_{Re}. Here a clear peak is observed in the vicinity of the phase transition. We associate this ''hard'' magnetic behavior with the expected structural disorder in the phase transition region.

Another useful quantity that can be extracted from the loops of Fig. 6 is the saturation Kerr effect $\Theta_{\mathrm{K}}^{\mathrm{sat}}$, defined as the difference between the maximum and minimum signals within each loop. This is plotted as a function of t_{Re} in Fig. 7(lower). $\Theta_{\mathrm{K}}^{\mathrm{sat}}$ is often assumed to be proportional to the magnetization density in studies of thin films. As such, we would expect $\Theta_{\mathrm{K}}^{\mathrm{sat}}$ to decrease with increasing t_{Re}, since the Fe magnetization is diluted by the addition of nonmagnetic Re.

We find that $\Theta_{\mathrm{K}}^{\mathrm{sat}}$ falls quickly to a minimum in the vicinity of the phase transition, followed by a slow rise in signal out to $t_{\mathrm{Re}}=35$ Å. From this we immediately conclude that the Fe retains a ferromagentic moment in the hcp region, justifying the main conclusion of this paper. But the detailed shape of $\Theta_{\mathrm{K}}^{\mathrm{sat}}$ suggests significant variations in the Fe magnetic moment with Re thickness. However, as we shall show below, the Fe moment is practically constant over the entire range of t_{Re}.

To understand the nonmonotonic behavior of Fig. 7 (lower), consider that $\Theta_{\mathrm{K}}^{\mathrm{sat}}$ is related to the magnetic moments of the individual layers as[13,14,12]

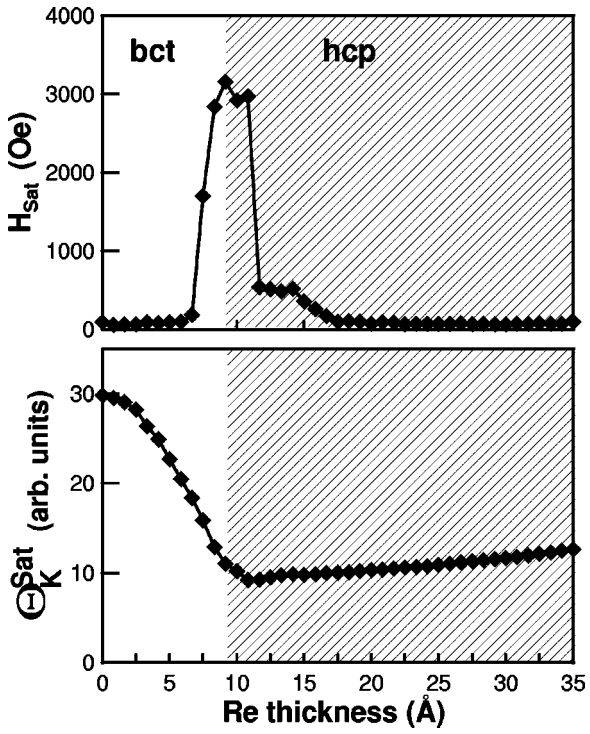

FIG. 7. Top: Saturation field, H_{sat} from the same Fe/Re multilayer over the t_{Re} range. H_{sat} exhibits a peak for 7 Å $<t_{\mathrm{Re}}<11$ Å, assocated with the phase transition region. Bottom: Saturation Kerr rotation $\Theta_{\mathrm{Kerr}}^{\mathrm{sat}}$ from Fe/Re multilayers over the Re thickness range. The overall Kerr rotation first decreases with increasing t_{Re}, reaching a minimum in the phase transition region. After the onset of the phase transition from bct to hcp structure at $t_{\mathrm{Re}}\approx 11$ Å, $\Theta_{\mathrm{K}}^{\mathrm{sat}}$ begins to increase slowly.

$$\Theta_{\mathrm{K}}^{\mathrm{sat}} \propto \frac{1}{t_{\mathrm{tot}}} \sum_i M_i t_i \xi_i \langle \mathrm{ME}_i \rangle. \tag{1}$$

Here M_i refers to the magnetic moments for Fe atoms in the interior part of each Fe layer (bulk part), Fe atoms at the Re interface, and any Re atoms which carry a magnetic moment. The spin-orbit coupling parameters ξ_i, matrix element factors $\langle \mathrm{ME}_i \rangle$,[15] and fractional thicknesses t_i have analogous meanings, while $t_{\mathrm{tot}}=\Sigma_i t_i$. In a simple approximation, we can consider that the ξ_i and matrix element factors in Eq. (1) are all equal between the different atom types. In this case, $\Theta_{\mathrm{K}}^{\mathrm{sat}}$ is proportional to the magnetization density of the film.[12]

Thus the shape of $\Theta_{\mathrm{K}}^{\mathrm{sat}}$ is expected to depart most strongly from the shape of the magnetization density curve when t_{Re} is small. When $t_{\mathrm{Re}}=0$ Å, almost all Fe atoms are in bulk-like environments, but when $t_{\mathrm{Re}}=2$ Å, a large proportion of Fe atoms are at the Re interface. The electron states of interfacial Fe atoms are changed, resulting in thickness-dependent matrix element factors in Eq. (1). However, after the Fe/Re interface is well established, say for $t_{\mathrm{Re}}=4$ Å, we expect the Fe matrix element factors to stop changing. Similarly, Re atoms near the Fe interface probably acquire a small magnetic moment and ξ_{Re} is many times larger than ξ_{Fe}, leading to a breakdown of proportionality between $\Theta_{\mathrm{K}}^{\mathrm{sat}}$ and magnetization density. However, this induced Re moment probably decays quickly away from the Fe interface, so

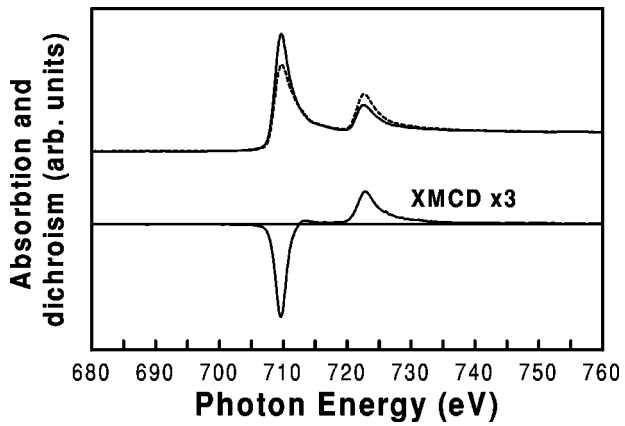

FIG. 8. X-ray absorption spectra (above) near the Fe $2p$ edge. As the magnetization direction is switched relative to the photon helicity, two absorption spectra are acquired. The difference of these two spectra is the XMCD (below). From the XMCD, we determine the Fe magnetic moment.

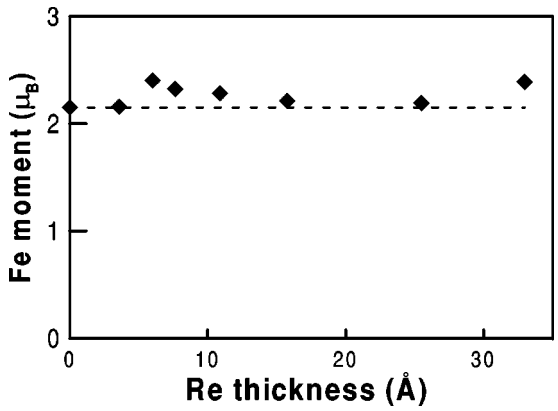

FIG. 9. Summary of the magnetic moment per Fe atom in Fe/Re multilayers as measured by XMCD. The dotted line through the Fe moments indicates the bulk value of Fe magnetic moment. Fe magnetic moment is roughly constant with t_{Re}.

that beyond $t_{\mathrm{Re}} \sim 10$ Å, the interior Re atoms no longer contribute to $\Theta_{\mathrm{K}}^{\mathrm{sat}}$.[16] Of course the phase transition will affect the Fe and Re matrix elements too. But the phase transition is essentially complete by $t_{\mathrm{Re}} \sim 12$ Å or so. From this analysis, the behavior of $\Theta_{\mathrm{K}}^{\mathrm{sat}}$ that is most difficult to explain is the increasing of $\Theta_{\mathrm{K}}^{\mathrm{sat}}$ with increasing t_{Re} beyond $t_{\mathrm{Re}} = 12$ Å. Beyond 12 Å, one would expect that transient phenomena discussed in the previous paragraph would have passed, and we should observe a monotonic dilution of magnetization with increasing t_{Re}. We speculate that small changes in the Fe structure might account for this. Near the phase transition, structural disorder reaches a maximum, and this has clear effects on $H_{95\%}$. Structural order improves beyond $t_{\mathrm{Re}} = 10$ Å. Furthermore, the overall lattice constant of the Fe/Re structure gradually approaches that of bulk Re and the Fe atoms presumably move farther apart. Perhaps these slight changes in structure affect the Fe matrix element factors, leading to an increase of $\Theta_{\mathrm{K}}^{\mathrm{sat}}$. Since the magnetic moment of hcp Fe is so strongly dependent on local environment, this appears to be a plausible explanation.

VI. XMCD EXPERIMENT

It is now well established that the magnitude of the XMCD is nearly proportional to the magnetic moment for a given element. This technique was first proposed by Erskine and Stern,[17] then realized by Schütz *et al.*[18] and measures differences in the circularly polarized x-ray absorption spectra depending on the relative orientation between the magnetic moment and photon helicity. XMCD measurements were performed at the Synchrotron Radiation Center in Madison, WI, using a UHV chamber (base pressure 1×10^{10} Torr). Samples were magnetized in 100 Oe fields along the easy axis and measured in a small field. The x-ray absorption spectra, obtained using a total yield technique, were normalized to the incident photon flux.

For Fe, XMCD is performed at the $2p$ absorption edge since this probes the $3d$ final states (which carry most of the magnetic moment). A typical Fe XMCD spectrum is displayed in Fig. 8. Here 85% circularly polarized x rays are incident on the film at 45° angle of incidence. The magnetization is switched at each photon energy by 180° in the sample plane. This generates two absorption spectra, with the magnetic moment either parallel or antiparallel to the projection of the photon helicity into the sample plane. The difference between these two spectra is the XMCD. The XMCD is approximately proportional to the Fe magnetic moment. Several XMCD spectra were taken at different points on the Fe/Re wedge from which the magnetic moment of the Fe is extracted. In order to accomplish this, the XMCD magnitude is extracted as a relative quantity by comparing a spectrum taken at the begining of the wedge (no Re) with spectra taken at other positions. The spectrum taken at the beginning of the wedge is then compared with that of a standard sample, in this case, a pure Fe film (see Refs. 19–21 for details of this procedure). The Fe moments thereby are deduced and corrected to saturation using the MOKE loops.

The Fe moments as measured by XMCD are summarized in Fig. 9. As can be seen, the Fe moment does not change by more than 9% from that of bulk Fe for any t_{Re}. This change is smaller than the systematic errors associated with the proportionality between XMCD and magnetic moment.[20,12] Hence we conclude that to within the errors inherent in XMCD measurements, the Fe magnetic moment is constant in the present films. Specifically, we observe no effect of the phase transition on the magnetic moment.

VII. DISCUSSION

From the x-ray analysis of the Fe/Re sputtered multilayers we found that the structure undergoes a phase transition from bct to hcp, which from a magnetic point of view leaves Fe unchanged. This is a surprising result, since based on previous literature[1,8,2,3,22–25,11] one would expect that after Fe is stabilized in hcp phase it will have no magnetic moment. This may be understood in the context of calculations performed by Abrikosov *et al.*[7] Their calculations reveal that though bulk hcp Fe has no moment at the equilibrium volume per atom, if this volume could somehow be increased by 20%, then Fe becomes once again a high spin metal with magnetic moment of $2.7\mu_B$. In our study at $t_{\mathrm{Re}} = 33$ Å, hcp

Fe was stabilized in Fe/Re multilayers with an average volume per atom $v_{avg}=14.57$ Å ^{3}/atom. This is 23% larger than the atomic volume of unstrained metastable fcc Fe (11.76 Å ^{3}), which should be quite close to the atomic volume of metastable hcp Fe. And indeed, in the present films the Fe is a ferromagnetic high spin metal.

Pushing this argument further, it is interesting to compare our samples with the Fe/Ru multilayers of Ref. 11. Bulk Ru has an atomic volume of $v_{Ru}=12.30$ Å ^{3}/atom. Thus, even if Fe were strained to match the lattice constant of Ru, it still would not have sufficient atomic volume to support a ferromagnetic moment, according to the above calculations. And indeed, those Fe/Ru multilayers were not ferromagnetic,[11] nor are any hcp FeRu alloys. Thus with a simple explanation related to the atomic volume, we can describe both the present results and previous studies as well.

VIII. CONCLUSIONS

Sputter deposited epitaxial Fe/Re multilayers were prepared. From XRD we have concluded that beyond a critical thickness of $t_{Re}\approx 9$ Å, these multilayers have an hcp structure. MOKE loops show that structural disorder in the vicinity of the bcc→hcp phase transition strongly affects the saturation field of the loops. However, the saturation Kerr effect does not drop to zero in the hcp region, as would be expected for paramagentic hcp Fe. XMCD enabled direct measurement of the Fe moment, and we found that in the present multilayers the Fe moment in the hcp region is quite close to that of bcc Fe. This is in strong distinction from previous studies of hcp Fe in the bulk, in alloys, or in multilayers. We attribute this difference to the greatly expanded lattice constant of hcp Fe in the present multilayers.

ACKNOWLEDGMENTS

The authors gratefully acknowledge support of the National Science Foundation CAREER Award No. DMR-9623246. The Synchrotron Radiation Center is supported by NSF under Award No. DMR-9212658.

[1] W. Keune, R. Halbauer, U. Gonsen, J. Lauer, and D. L. Williamson, J. Appl. Phys. **8**, 2976 (1977).
[2] C. S. Wang, B. M. Klein, and H. Krakauer, Phys. Rev. Lett. **54**, 1852 (1985).
[3] V. L. Moruzzi, P. M. Marcus, K. Schwarz, and P. Mohn, Phys. Rev. B **34**, 1784 (1986).
[4] For a recent review discussing experimental studies of fcc Fe films, see G. R. Harp, in *Thin Film: Heteroepitaxial Systems*, edited by W. K. Liu and M. B. Santos (World Scientific, Singapore, 1999).
[5] L. Del Bianco, C. Ballesteros, J. M. Rojo, and A. Hernando, Phys. Rev. Lett. **81**, 4500 (1998).
[6] T. Asada and K. Terakura, Phys. Rev. B **46**, 13 599 (1992).
[7] I. A. Abrikosov, P. James, O. Eriksson, P. Söderlind, A. V. Ruban, H. L. Skriver, and B. Johansson, Phys. Rev. B **54**, 3380 (1996).
[8] R. D. Taylor, G. Cort, and J. O. Willis, J. Appl. Phys. **53**, 8199 (1982).
[9] D. I. C. Pearson and J. M. Williams, J. Phys. F: Met. Phys. **9**, 1797 (1979).
[10] F. Baudelet, A. Fontaine, G. Tourillon, D. Guay, M. Maurer, M. Piecuch, M. F. Ravet, and V. Dupuis, Phys. Rev. B **47**, 2344 (1993).
[11] T. Lin, M. A. Tomaz, M. M. Schwickert, and G. R. Harp, Phys. Rev. B **58**, 862 (1998).
[12] G. R. Harp, F. Perjeru, M. M. Schwickert, W. Antel, and Tao Lin (unpublished).
[13] P. Bruno, in *Magnetismus von Festkörpern und Grenzflächen, Ferienkurse des Forschungszentrums* (KFA Jülich, Jülich, 1993).
[14] D. Weller, G. R. Harp, R. F. C. Farrow, A. Cebollada, and J. Sticht, Phys. Rev. Lett. **72**, 2097 (1994).
[15] This so called ''matrix element'' factor is a complicated quantity which couples the occupied and unoccupied electron states within the multilayer via the Hamiltonian of the optical wavefield. For our purposes it is just a number, although this number may be dependent on the value of t_{Re}. See Ref. 14, and references therein, for details.
[16] We were not able to measure the induced Re magnetic moments in these multilayers, as by XMCD. The present supposition is supported by analogy with numerous other Fe/transition metal (TM) systems where the induced TM moment could be measured (Ref. 12).
[17] J. L. Erskine and E. A. Stern, Phys. Rev. B **12**, 5016 (1975).
[18] G. Schütz, W. Wagner, W. Wilhelm, P. Keinle, R. Zeller, R. Frahm, and G. Materlik, Phys. Rev. Lett. **58**, 737 (1987).
[19] M. A. Tomaz, W. J. Antel, and G. R. Harp, Bull. Am. Phys. Soc. **41**, 490 (1996).
[20] T. Lin, W. J. Antel, Jr., W. L. O'Brien, and G. R. Harp, Phys. Rev. B **55**, 3716 (1997).
[21] T. Lin, M. M. Schwickert, M. A. Tomaz, H. Chen, and G. R. Harp, Phys. Rev. B **59**, 13 911 (1999).
[22] D. Pescia, M. Stampanoni, G. L. Bona, A. Vaterlaus, R. F. Willis, and F. Meier, Phys. Rev. Lett. **58**, 2126 (1987).
[23] D. Tian, F. Jona, and P. M. Marcus, Phys. Rev. B **45**, 11 216 (1992).
[24] D. Li, M. Freitag, J. Pearson, Z. Q. Qiu, and S. D. Bader, Phys. Rev. Lett. **72**, 3112 (1994).
[25] S. Müller, P. Bayer, C. Reischl, and K. Heinz, Phys. Rev. Lett. **74**, 765 (1995).